frontiers in Microbiology

ORIGINAL RESEARCH
published: 09 March 2022
doi: 10.3389/fmicb.2022.807014

UPLC-Q-TOF-MS/MS Analysis of *Seco*-Sativene Sesquiterpenoids to Detect New and Bioactive Analogues From Plant Pathogen *Bipolaris sorokiniana*

Yan-Duo Wang[1†], Jian Yang[2†], Qi Li[1], Yuan-Yuan Li[1], Xiang-Mei Tan[1], Si-Yang Yao[3], Shu-Bin Niu[3], Hui Deng[4], Lan-Ping Guo[2] and Gang Ding[1]**

[1] Key Laboratory of Bioactive Substances and Resources Utilization of Chinese Herbal Medicine, Ministry of Education, Institute of Medicinal Plant Development, Chinese Academy of Medical Sciences and Peking Union Medical College, Beijing, China, [2] State Key Laboratory Breeding Base of Dao-di Herbs, National Resource Center for Chinese Materia Medica, China Academy of Chinese Medical Sciences, Beijing, China, [3] Department of Pharmacy, Beijing City University, Beijing, China, [4] Key Laboratory of Microbial Resources, Ministry of Agriculture and Rural Affairs, Institute of Agricultural Resources and Regional Planning, Chinese Academy of Agricultural Sciences, Beijing, China

Seco-sativene sesquiterpenoids are an important member of phytotoxins and plant growth regulators isolated from a narrow spectrum of fungi. In this report, eight *seco*-sativene sesquiterpenoids (**1**–**8**) were first analyzed using the UPLC-Q-TOF-MS/MS technique in positive mode, from which their mass fragmentation pathways were suggested. McLafferty rearrangement, 1,3-rearrangement, and neutral losses were considered to be the main fragmentation patterns for the $[M+1]^+$ ions of **1**–**8**. According to the structural features (of different substitutes at C-1, C-2, and C-13) in compounds **1**–**8**, five subtypes (A–E) of *seco*-sativene were suggested, from which subtypes A, B/D, and E possessed the diagnostic daughter ions at *m/z* 175, 189, and 203, respectively, whereas subtype C had the characteristic daughter ion at *m/z* 187 in the UPLC-Q-TOF-MS/MS profiles. Based on the fragmentation patterns of **1**–**8**, several known compounds (**1**–**8**) and two new analogues (**9** and **10**) were detected in the extract of plant pathogen fungus *Bipolaris sorokiniana* based on UPLC-Q-TOF-MS/MS analysis, of which **1**, **2**, **9**, and **10** were then isolated and elucidated by NMR spectra. The UPLC-Q-TOF-MS/MS spectra of these two new compounds (**9** and **10**) were consistent with the fragmentation mechanisms of **1**–**8**. Compound **1** displayed moderate antioxidant activities with IC_{50} of 0.90 and 1.97 mM for DPPH and $ABTS^+$ scavenging capacity, respectively. The results demonstrated that *seco*-sativene sesquiterpenoids with the same subtypes possessed the same diagnostic daughter ions in the UPLC-Q-TOF-MS/MS profiles, which could contribute to structural characterization of *seco*-sativene sesquiterpenoids. Our results also further supported that UPLC-Q-TOF-MS/MS is a powerful and sensitive tool for dereplication and detection of new analogues from crude extracts of different biological origins.

Keywords: *Bipolaris sorokiniana*, *seco*-sativene sesquiterpenoids, McLafferty rearrangement, NMR analysis, antioxidant activity

OPEN ACCESS

Edited by:
Mukesh Kumar Awasthi,
Northwest A&F University, China

Reviewed by:
Hayssam M. Ali,
King Saud University, Saudi Arabia
Ali Raza,
Shanghai Jiao Tong University, China
Ramprasad E.V.V.,
University of Hyderabad, India
Haiyang Xia,
Taizhou University, China
Qing Du,
Tsinghua University, China

****Correspondence:***
Lan-Ping Guo
glp01@126.com
Gang Ding
dgfyhchina@163.com;
gding@implad.ac.cn

[†] These authors have contributed equally to this work and share first authorship

Specialty section:
This article was submitted to Microbiotechnology, a section of the journal Frontiers in Microbiology

Received: *03 November 2021*
Accepted: *27 January 2022*
Published: *09 March 2022*

Citation:
Wang Y-D, Yang J, Li Q, Li Y-Y, Tan X-M, Yao S-Y, Niu S-B, Deng H, Guo L-P and Ding G (2022) UPLC-Q-TOF-MS/MS Analysis of Seco-Sativene Sesquiterpenoids to Detect New and Bioactive Analogues From Plant Pathogen Bipolaris sorokiniana. Front. Microbiol. 13:807014. doi: 10.3389/fmicb.2022.807014

INTRODUCTION

Seco-sativenes are a member of sesquiterpenoids possessing a unique bicyclo[3.2.1]octane ring system and different substitutions including glycosylation, methylation, and acylation; different heterocyclic rings such as lactone, furan, and pyran ring; and diverse oxygenation sites (hydroxylation) on the core skeleton, increasing the chemical diversity. The structural differences of *seco*-sativenes mainly lie in the diverse substituents at C-1, C-2, and C-13 (Li et al., 2020a). From the structural features, it is implied that *seco*-sativenes come from a sesquiterpene pathway but not from a direct farnesyl pyrophosphate cyclization product. Rearrangement and oxidative cleavage reactions might play a pivotal role in the biosynthetic pathway, which is supported by the isolation of different precursors and intermediates (Mayo et al., 1962a, 1965; Mayo and Williams, 1965; Li et al., 2020a,b). Fungus *B. sorokiniana* is known for producing a variety of secondary metabolites, with sesterterpene, cyclic peptides, and sesquiterpenoids as the most representative classes (Nihashi et al., 2002; Ali et al., 2016; Qader et al., 2017; Phan et al., 2019). Qader et al. (2017) isolated three *seco*-sativene sesquiterpenoids from *B. sorokiniana*, in which helminthosporal acid and helminthosporol displayed a strong phytotoxic effect on lettuce seed germination and toxicity against brine shrimps, and helminthosporal acid also showed antifungal activity. Phan et al. (2019) isolated and elucidated 12 *seco*-sativene sesquiterpenoids including a new *seco*-sativene sesquiterpenoid and three new sativene analogues from *B. sorokiniana*, in which helminthosporic acid and dihydroprehelminthosporol displayed weak necrotic activity against wheat leaves and helminthosporol showed an inhibitory effect on seed germination. *Seco*-sativene analogues displayed strong phytotoxic effects on cereals and gramineous plants, (Ludwig et al., 1956; Ludwig, 1957; Mayo et al., 1961, 1962b, 1963; Spencer, 1965; Katsumi et al., 1967; Taniguchi and White, 1967; White and Taniguchi, 1972; Pena-Rodriguez et al., 1988; Pena-Rodriguez and Chilton, 1989; Qader et al., 2017; Phan et al., 2019) whereas others possessed plant-growth-promoting biological activities to rice, lettuce, cucumber, and wheat seedlings (Briggs, 1966; Hashimoto et al., 1967; Nukina et al., 1975; Pena-Rodriguez and Chilton, 1989; Miyazaki et al., 2017, 2018; Qader et al., 2017). In addition, some *seco*-sativene sesquiterpenoids also possessed antifungal, cytotoxic, and toxic effects, and other analogues could inhibit the growth of the malaria-causing protozoan of *Plasmodium falciparum* and exhibited certain anti-NO production activities (Li et al., 2020b). The novel core skeleton and diverse biological activities attracted us to chemically investigate this unique member of sesquiterpenoids. Recently, a series of new *seco*-sativene sesquiterpenoids were isolated from the endophytic fungus *Cochliobolus sativus* (teleomorph: *Bipolaris sorokiniana*) inhabiting in a desert plant, *Artemisia desertorum*, and their structures were mainly determined by NMR experiments, X-ray diffraction, and high-resolution mass analysis. Helminthosporic acid (**2**) could promote plant leaf growth, whereas cochliobolin F, helminthosporic acid (**2**), drechslerine B (**8**), and helminthosporal acid displayed strong phytotoxic effects on corn leaves (Li et al., 2020a). However, the traditional isolation method was used as the main technique for the isolation of *seco*-sativene sesquiterpenoids, (Ramos et al., 2019) which precluded discovery of new/novel analogues of *seco*-sativene sesquiterpenoids. Thus, efficient approaches for mining novel structures of *seco*-sativene sesquiterpenoids are urgent.

Mass spectrometry, especially tandem mass spectrometry, has been one of the most important physicochemical approaches for the characterization of secondary metabolites due to its rapidity and sensitivity (Jin et al., 2018; Liang et al., 2018; Conceição et al., 2020; Scupinari et al., 2020). Molecular weight and formula are often inconclusive for metabolite identification; however, fragmentation patterns represent a specific feature for a certain structural class. Chen et al. (2018) applied neutral loss scan in QqQ-MS and molecular formula calculation in UPLC-Q-TOF-MS to detect amorfrutin analogues, which provided the idea of detection and structural dereplication in the complex crude extract. Yang et al. (2017) used UPLC-Q-TOF-MS/MS coupled with neutral loss scan and diagnostic ions to analyze the secondary metabolites of *Schisandra chinensis*. Ahad et al. (2020) combined UPLC-Q-TOF-MS with SCX-SPE to achieve the enrichment and structural identification of the same skeleton metabolites. Thus, much evidence demonstrated that fragmentation patterns coupled with UPLC-Q-TOF-MS/MS analysis were an efficient and convenient tool for the detection and dereplication of similar metabolites.

A series of *seco*-sativene sesquiterpenoids (**1–8**, **Figure 1**) were isolated and elucidated in our previous work (Li et al., 2020a). According to the structural features (of different groups at C-1, C-2, and C-13), five subtypes of *seco*-sativenes were suggested (subtypes A-E) (**Figure 1**). Interestingly, each subtype of the structure has the same diagnostic daughter ions in the mass spectrometric profile, which could provide a reliable approach to analyze structures of *seco*-sativenes and target potent new analogues. To date, no investigations about electrospray tandem mass/mass of *seco*-sativenes sesquiterpenoids were reported. The potential application prospect and unique skeleton of *seco*-sativenes prompted us to investigate the mass spectrometric cleavage mechanisms of this unique member of sesquiterpenoids.

In this report, the UPLC-Q-TOF-MS/MS fragmentation rules of *seco*-sativene sesquiterpenoids (**1–8**) were presented; some known and new *seco*-sativene sesquiterpenoids were detected from the extract of the plant pathogen fungus *Bipolaris sorokiniana* based on UPLC-Q-TOF-MS/MS analysis. Two new (**9** and **10**) and two known (**1** and **2**) *seco*-sativene sesquiterpenoids were then isolated and elucidated by HR-ESI-MS and NMR spectra, and the antioxidant activities of these *seco*-sativene sesquiterpenoids (**1, 2, 9**, and **10**) were assessed.

MATERIALS AND METHODS

General Experimental Procedures

Optical rotations were measured on a 241 polarimeter (PerkinElmer, Waltham, United States). UV-2102 (Unico, Shanghai, China) was used to record UV data. IR spectra were recorded on an FTIR-8400S spectrophotometer (Shimadzu, Kyoto, Japan). NMR data were acquired on a Bruker 500

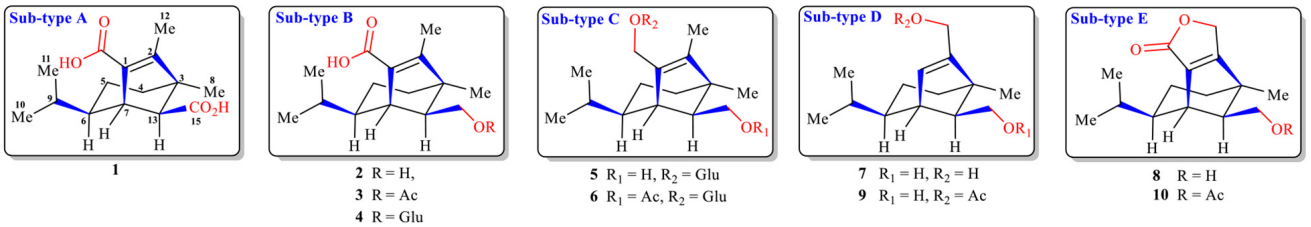

FIGURE 1 | Structures of *seco*-sativene sesquiterpenoids (**1–10**).

TABLE 1 | NMR spectroscopic data of compounds **9** and **10** in $CDCl_3$.

Pos.	9					10				
	$\delta_H{}^a$ (*J* in Hz)	$\delta_C{}^b$, mult.	^{1}H-^{1}H COSY	HMBC	NOESY	$\delta_H{}^a$ (*J* in Hz)	$\delta_C{}^b$, mult.	^{1}H-^{1}H COSY	HMBC	NOESY
1	5.64, s	127.5, CH	H7	C3, C6, C12, C13			134.8, C		H7, H12, H13	
2		141.0, C		H4, H7, H8, H12, H13			177.2, C		H4, H7, H8, H12, H13	
3		47.0, C		H1, H4, H5, H7, H8, H12, H13, H14			46.9, C		H4, H5, H7, H8, H13, H14	
4	1.36, ddd (13.5, 6.5, 1.5)	34.5, CH_2	H5	C2, C3, C5, C6, C8, C13		1.57, m	34.5, CH_2	H15	C2, C3, C5, C6, C8, C13	
	1.29, m									
5	1.67, m	25.1, CH_2	H4, H6	C3, C4, C6		1.89, m	25.8, CH_2	H4, H6	C3, C4, C6, C7	
	1.11, m					0.89, m				
6	1.09, m	43.9, CH	H7	C4, C7, C10, C11, C13	H13	1.21, m	43.8, CH	H5, H7, H9	C9, C10, C11	H13
7	2.70, s	42.2, CH	H6, H13	C3, C5, C6, C9, C13, C14	H10	3.04, s	41.0, CH	H1, H6, H13	C1, C2, C3, C5, C6, C14	H10
8	1.01, s	18.6, CH_3		C2, C3, C4, C13		1.16, s	18.1, CH_3		C2, C3, C4, C13	
9	1.21, dtd (13.5, 6.5, 2.0)	32.5, CH	H6, H10, H11	C5, C6, C10, C11		1.26, m	32.4, CH	H6, H10, H11	C5, C6, C10, C11	
10	0.93, d (6.5)	21.2, CH_3	H9, H11	C6, C9, C11	H7	1.04, d (6.0)	21.5, CH_3	H9, H11	C6, C9, C11	H7
11	0.83, d (6.5)	20.8, CH_3	H9, H10	C6, C9, C10		0.83, d (6.0)	20.7, CH_3	H9, H10	C6, C9, C10	
12	4.59, d (13.5)	62.9, CH_2		C1, C2, C3, C2′		4.83, dd (18.0, 1.5)	67.5, CH_2		C1, C2	
	4.52, d (13.5)					4.73, d (18.0)				
13	1.57, dd (8.5, 5.0)	62.6, CH	H7, H14	C1, C2, C3, C4, C6, C14	H6	2.16, dd (9.0, 5.5)	63.5, CH	H7, H14	C1, C2, C3, C4, C6, C14	H6
14	3.73, dd (10.5, 5.0)	63.0, CH_2	H13	C3, C7, C13		4.24, dd (11.0, 5.5)	64.0, CH	H13	C3, C7, C13, C2′	
	3.50, dd (10.5, 8.0)					3.82, dd (11.0, 9.0)				
15							170.8, C		H12	
1′	2.07, s	21.0, CH_3		C12, C2′		2.05, s	21.2, CH_3		C14, C2′	
2′		171.2, C		H12, H1′			171.2, C		H14, H1′	

[a] *Recorded at 500 MHz.*
[b] *Recorded at 125 MHz.*

spectrometer using solvent signal ($CDCl_3$; δ_H 7.26/δ_C 77.6) as reference. Sephadex LH-20 and silica gel were purchased from Pharmacia (Biotech, Sweden) and Shanghai Titan Scientific Co., Ltd. (Shanghai, China), respectively. Semi-preparative HPLC separation was performed on a SEP LC-52 with an MWD UV detector (Separation (Beijing) Technology Co Ltd., Beijing, China) packed with a YMC-Pack ODS-A column. HR-ESI-MS spectra were analyzed using an ESI-Q-TOF-MS (Waters Xevo G2-XS QTof, United States).

General Experimental Procedures

Eight *seco*-sativene sesquiterpenoids were analyzed using a UPLC-Q-TOF-MS/MS system (Waters, United States). Chromatographic analysis was carried out with a Waters ACQUITY UPLC-PDA system equipped with an analytical reverse-phase C-18 column (2.1 × 100 mm, 1.7 μm, ACQUITY BEH, Waters, United States) with an absorbance range of 200 to 400 nm. The column temperature was maintained at 40°C. As the mobile phase, 0.1% formic acid in water (A) and 0.1% formic acid in acetonitrile (B) were used. The gradient conditions were as follows: 0–2 min, 35% B; 2–17 min, 35–98% B; 17–19 min, 98% B; and 19.1–21 min, 35% B. The flow rate from the UPLC system into the ESI-Q-TOF-MS detector was 0.3 ml/min. The auto-injected volume was 0.3 μl. Time-of-flight MS detection was performed with the Xevo G2-XS QTof system (Waters) combined with an ESI source in positive ion scan mode. The desolvation temperature was set at 450°C with desolvation gas flow at 900 L/h, and the source

TABLE 2 | Elemental constituents of major product ions from $[M+Na]^+$ for compound **1** (subtype A).

Fragment ion	Formula	Calculated	Observed	Error (PPM)
$[M+Na]^+$	$C_{15}H_{22}O_4Na$	289.1416	289.1412	−1.4
$[M+H-H_2O]^+$	$C_{15}H_{21}O_3$	249.1491	249.1499	+3.2
$[M+H-2H_2O]^+$	$C_{15}H_{19}O_2$	231.1385	231.1378	−3.0
$[M+H-H_2O-CO]^+$	$C_{14}H_{21}O_2$	221.1542	221.1537	−2.3
$[M+H-H_2O-HCO_2H]^+$	$C_{14}H_{19}O$	203.1436	203.1429	−3.4
$[M+H-H_2O-HCO_2H-CO]^+$	$C_{13}H_{19}$	175.1487	175.1479	−4.6

temperature was 80°C. The lock mass in all analyses was leucine-enkephalin $[(M+H)^+ = 556.2771]$, used at a concentration of 200 μl/ml and infused at a flow rate of 10 L/min. Raw data were acquired using the centroid mode, and the mass range was set from *m/z* 100 to 1,000. The capillary voltage was set at 2.5 kV with 30 V of sample cone voltage. The collision energy was set as 6 eV for low-energy scan and a ramp from 30 to 50 eV for high-energy scan. The instrument was controlled by MassLynx 4.1 software.

Strain and Fermentation

The strain of *Bipolaris sorokiniana* (strain number: ACCC36805) was isolated from the seed of wheat and provided by the Chinese Academy of Agricultural Sciences. The fungus was grown on PDA (potato dextrose agar) plates at 25°C for 10 days. Then the fresh mycelium was inoculated into the autoclaving sterilized solid medium with the formula of rice (60.0 g) and distilled water (80 ml) in Fernbach flasks (500 ml) for further fermentation at 25°C for 30 days.

Extraction and Isolation

The fermented rice substrate was extracted with EtOAc three times, and the solvent was evaporated to dryness under vacuum to afford 200 g of crude extract. The original extract was fractionated on a silica gel column using petroleum ether-acetone (1:0–0:1) progressively to give five fractions (Fr. 1 to Fr. 5). Fr. 2 (8.0 g) was separated on a silica gel column to obtain eight fractions (Fr. 2.1 to Fr. 2.8). Fr. 4 (27.8 g) was separated on a silica gel column to obtain five parts (Fr. 4.1 to Fr. 4.5). Fr. 4.1 was separated on a silica gel column and RP-HPLC (0–5 min 80% MeOH in H_2O, 5–25 min 80–100% MeOH in H_2O, 5 ml/min) to obtain Fr. 4.1.1 (13.8 mg, t_R = 10.5 min). Fr. 4.1.1 (13.8 mg) was purified by semi-preparative HPLC (0–5 min 70% acetonitrile in H_2O, 5–25 min 70–90% acetonitrile in H_2O, 2 ml/min) to obtain compound **10** (1.8 mg, t_R = 15.2 min). Fr. 4.2 (5.6 mg) was purified by semi-preparative HPLC (60% acetonitrile in H_2O, 2.5 ml/min) to obtain compound **9** (2.3 mg, t_R = 23.5 min). Fr. 4.3 (3.5 g) was purified by semi-preparative HPLC (0–25 min 80–100% MeOH in H_2O, 5 ml/min) to obtain compound **2** (230.1 mg, t_R = 10.3 min). Fr. 4.4 (4.02 g) was separated on a silica gel column, Sephadex LH-20 (dichloromethane:methanol = 1:1 v/v) and semi-preparative HPLC to obtain four fractions (Fr. 4.4.1–Fr. 4.4.4). Fr. 4.4.1 (24.7 mg) was purified by semi-preparative HPLC (75% MeOH in H_2O, 2 ml/min) to obtain **1** (10.0 mg, 21.6 min).

12-Acetyl-Drechslerine A (9)

Colorless oil: $[\alpha]_{25}^{D}$-18 (c 0.1, MeOH); UV (MeOH) λ_{max} (log ε) 215 (2.98) nm; IR (neat) ν_{max} 3,420, 2,931, 1,742, 1,456, 1,367, 1,235, 1,031 cm^{-1}; for ^1H NMR and ^{13}C NMR data, see **Table 1**; positive HR-ESI-MS: *m/z* 267.1957 [calcd. for $C_{16}H_{27}O_3$ $[M+H]^+$, 267.1960].

14-Acetyl-Drechslerine B (10)

White powder: $[\alpha]_{25}^{D}$-16 (c 0.1, MeOH); UV (MeOH) λ_{max} (log ε) 205 (2.84), 234 (2.97) nm; IR (neat) ν_{max} 2,958, 1,747, 1,645, 1,456, 1,367, 1,338, 1,234, 1,031 cm^{-1}; for ^1H NMR and ^{13}C NMR data, see **Table 1**; positive HR-ESI-MS: *m/z* 293.1683 [calcd. for $C_{17}H_{25}O_4$ $[M+H]^+$, 293.1675].

Antioxidant Activity

DPPH Scavenging Capacity

Take 15 μl of compounds **1**, **2**, **9**, and **10** with a concentration of 10 mM/L and a serial dilution of seven times, and then mix

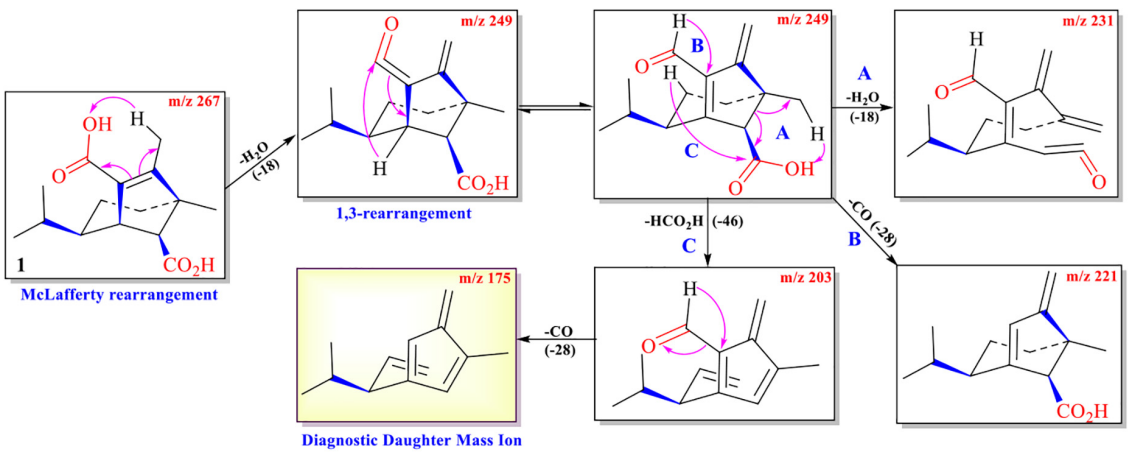

SCHEME 1 | Possible fragmentation pathway of **1**.

TABLE 3 | Elemental constituents of major product ions from $[M+Na]^+$ for compound **2** (subtype B).

Fragment ion	Formula	Calculated	Observed	Error (PPM)
$[M+Na]^+$	$C_{15}H_{24}O_3Na$	275.1623	275.1618	−1.8
$[M+H]^+$	$C_{15}H_{25}O_3$	253.1804	253.1797	−2.8
$[M+H-H_2O]^+$	$C_{15}H_{23}O_2$	235.1698	235.1703	+2.1
$[M+H-2H_2O]^+$	$C_{15}H_{21}O$	217.1592	217.1582	−4.6
$[M+H-2H_2O-CO]^+$	$C_{14}H_{21}$	189.1643	189.1631	−6.3

with DPPH solution. After 30 min, the remaining amount of the DPPH radical was measured spectrophotometrically at 517 nm. In this test, for comparison, V_C was considered as the positive control, and ethanol was considered as the negative control.

The clearance rate E is $E = [1 - (A_S - A_0)/(A_C - A_0)] \times 100\%$, where A_0 is the absorbance of the water, A_C is the absorbance of ethanol solution, and A_S is the absorbance after adding the sample solution. The IC_{50} value was processed by GraphPad Prism 8.

$ABTS^+$ Scavenging Capacity

Take 15 μl of compounds **1**, **2**, **9**, and **10** with a concentration of 10 mM/L and a serial dilution of seven times, and then mix with $ABTS^+$ solution. After 6 min, the remaining amount of the $ABTS^+$ radical was measured spectrophotometrically at 405 nm. In this test, for comparison V_C served as the positive control, and ethanol served as the negative control.

The clearance rate E is $E = [1 - (A_S - A_0)/(A_C - A_0)] \times 100\%$, where A_0 is the absorbance of the water, A_C is the absorbance of ethanol solution, and A_S is the absorbance after adding the sample solution. The IC_{50} value was processed by GraphPad Prism 8.

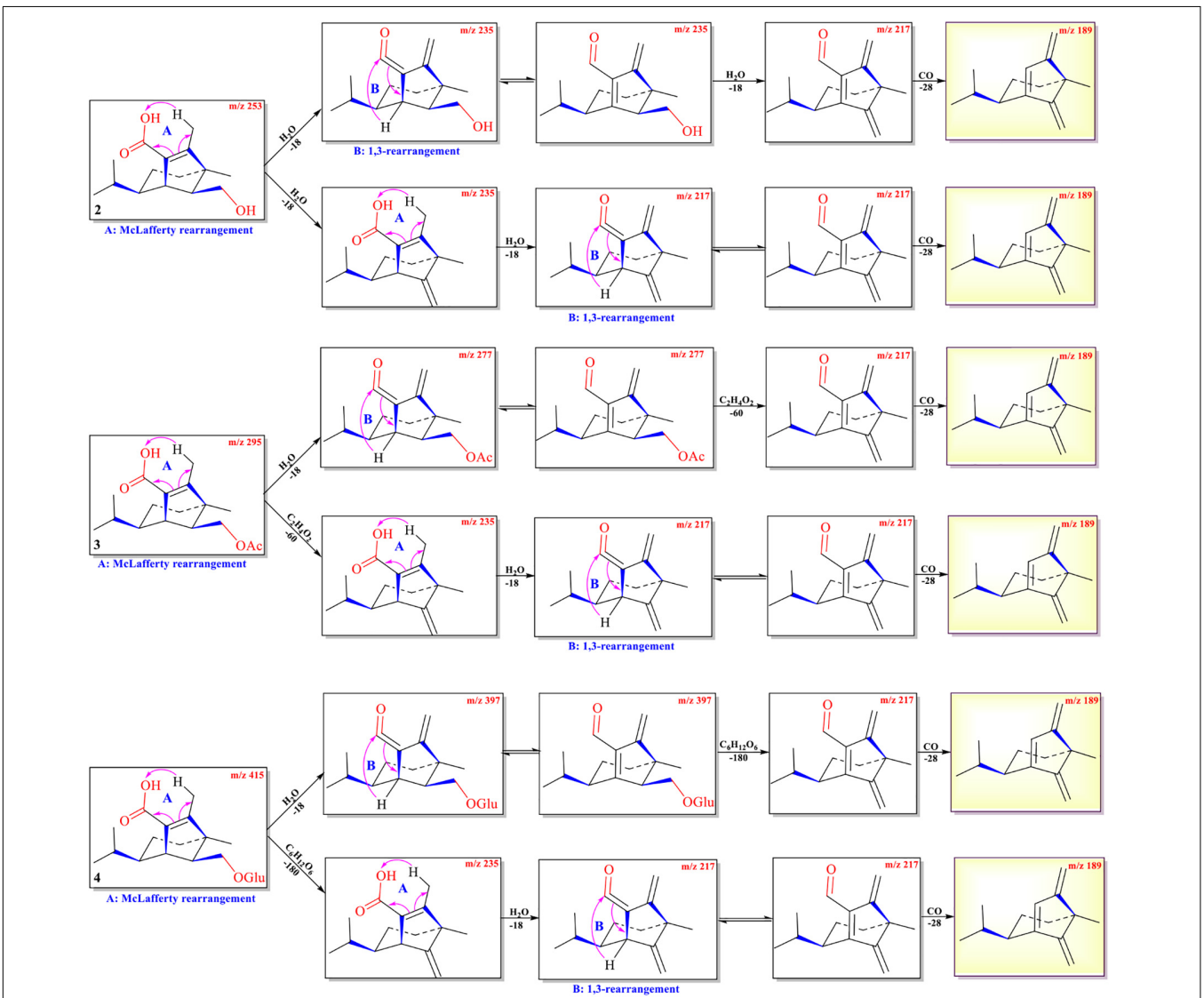

SCHEME 2 | Possible fragmentation pathways of **2**–**4**.

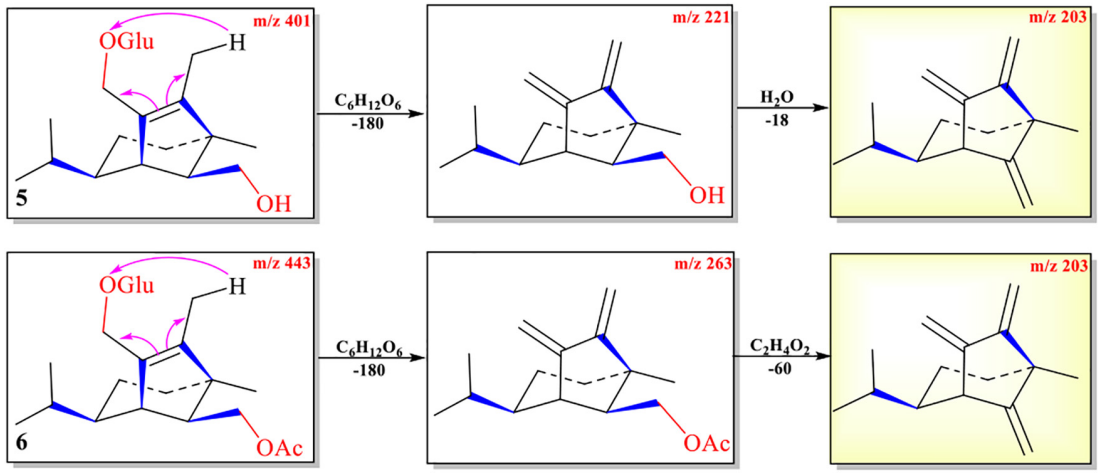

SCHEME 3 | Possible fragmentation pathways of **5** and **6**.

RESULTS

Fragmentation Mechanisms of *Seco*-Sativene Sesquiterpenoids (1–8)

The protonated parent ion *m/z* 267, $[M+H]^+$ of cochliobolin A (**1**) was not observed in the UPLC-Q-TOF-MS/MS spectra, and it might be that this ion could easily lose one molecule of H_2O to produce a daughter ion at *m/z* 249 $[M+1\text{-}H_2O]^+$. The abundance of ion *m/z* 249 was the highest in the profile. Thus, the precursor protonic molecular ion $[M+1\text{-}H_2O]^+$ of **1** was selected for analysis in the UPLC-Q-TOF-MS/MS spectrum. The high-resolution mass and fragment ions together with the elemental constituents of cochliobolin A (**1**) were listed in **Table 2**. The fragmentation routes according to ESI-Q-TOF-MS/MS analysis were depicted in **Scheme 1**, in which typical neutral losses, McLafferty rearrangement, and 1,3-rearrangement were the main fragmentation patterns for the parent ion *m/z* 267 [M+1]+ (Liang et al., 2018). The daughter ion (*m/z* 249) was formed from the parent ion (*m/z* 267) through the McLafferty rearrangement and 1,3 rearrangement by loss of one molecule of H_2O (−18). Then, the daughter ion (*m/z* 221) was produced from the precursor ion (*m/z* 249) through neutral loss of one molecule of CO (−28). The daughter ion (*m/z* 231) was yielded from the precursor ion (*m/z* 249) through the McLafferty rearrangement by neutral loss of one molecule of H_2O (−18). The diagnostic daughter ion (*m/z* 175) might have originated from the precursor ion (*m/z* 249) by loss of one molecule of HCO_2H (−46) (*m/z* 203) and one molecule of CO (−28) (*m/z* 175) through the McLafferty rearrangement and neutral loss (**Scheme 1** and **Supplementary Figure 1**).

The protonated parent ion *m/z* 253, $[M+H]^+$ of compound **2** was observed in the mass profile with a relatively low abundance, which easily lost one molecule of H_2O (−18) to produce the intermediate ion *m/z* 235 through the McLafferty rearrangement and 1,3-rearrangement or neutral loss of one molecule of H_2O (–18) with H-13. Then, the intermediate ion *m/z* 235 successively lost one molecule of H_2O (–18) and one molecule of CO (–28) by neutral loss to form the key diagnostic daughter ion (*m/z* 189). The high-resolution mass and fragment ions together with the elemental constituents of compound **2** were listed in **Table 3**. Compounds **3** and **4** had similar fragmentation pathways to that of compound **2** (**Scheme 2**, **Supplementary Figures 2–4**, and **Supplementary Tables 1, 2**).

The protonated parent ions of **5** and **6** were *m/z* 401 $[M+H]^+$ and *m/z* 443 $[M+H]^+$, respectively, in the UPLC-Q-TOF-MS/MS spectra. These two ions lost one molecule of glucose (–180) by the McLafferty rearrangement to form the intermediate ions *m/z* 221 and *m/z* 263, respectively, which yielded the same diagnostic ion *m/z* 203 through neutral loss of one molecule of H_2O (−18) and one molecule of CH_3COOH (−60) (**Scheme 3** and **Supplementary Figures 5, 6**). The high-resolution mass and fragment ions together with the elemental constituents of compounds **5** and **6** were listed in **Table 4** and **Supplementary Table 3**.

The abundance of protonated parent ion of **7** *m/z* 225 $[M+H]^+$ was relatively low in the UPLC-Q-TOF-MS/MS spectra. It might be the neutral loss of one molecule of H_2O (−18) and one molecule of CH_3CO_2H (−60) to form an intermediate ion *m/z* 207. The abundance of the ion (*m/z* 207) was the highest in the mass profile. The diagnostic ion (*m/z* 189) was formed from ion *m/z* 207 by loss of one molecule of H_2O (−18) through the McLafferty rearrangement (**Scheme 4** and **Supplementary Figure 7**). The high-resolution mass and fragment ions together

TABLE 4 | Elemental constituents of major product ions from $[M+Na]^+$ for compound **5** (subtype C).

Fragment ion	Formula	Calculated	Observed	Error (PPM)
$[M+Na]^+$	$C_{21}H_{36}O_7Na$	423.2359	423.2361	+0.5
$[M+H]^+$	$C_{21}H_{37}O_7$	401.2539	401.2535	−1.0
$[M+H\text{-}C_6H_{12}O_6]^+$	$C_{15}H_{25}O$	221.1905	221.1901	−1.8
$[M+H\text{-}C_6H_{12}O_6\text{ -}H_2O]^+$	$C_{15}H_{23}$	203.1800	203.1790	−4.9

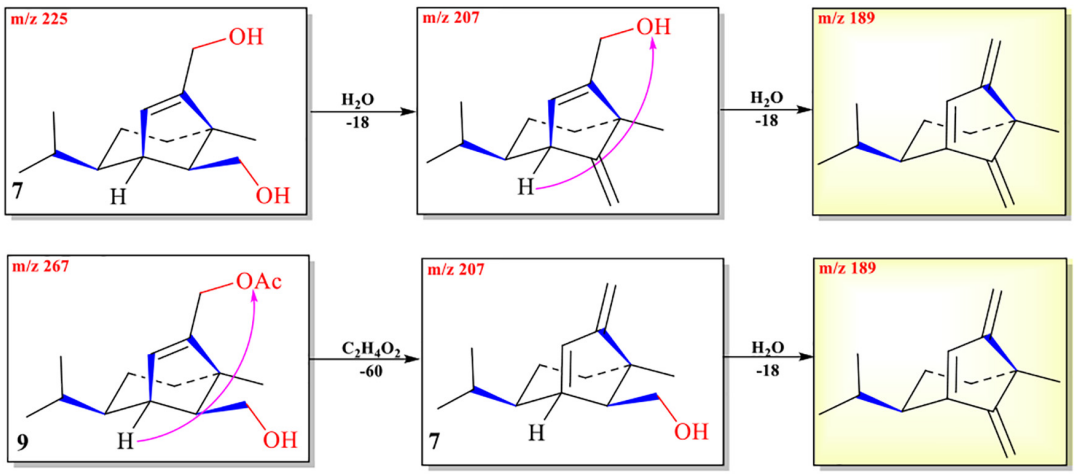

SCHEME 4 | Possible fragmentation pathways of **7** and **9**.

with the elemental constituents of compound **7** are listed in **Table 5**.

The protonated parent ion of **8** was *m/z* 251 $[M+H]^+$ in the UPLC-Q-TOF-MS/MS spectra with the highest abundance. The McLafferty rearrangement produced the intermediate ion *m/z* 233 from *m/z* 251 by loss of one molecule of H_2O (−18). Successive neutral losses of one molecule of H_2O (−18) and one molecule of CO (−28) or vice versa yielded the diagnostic daughter ion (*m/z* 187). The detailed MS analysis is shown in **Scheme 5** and **Supplementary Figure 8**. The high-resolution mass and fragment ions together with the elemental constituents of compound **8** are listed in **Table 6**.

With the UPLC-Q-TOF-MS/MS fragmentation mechanisms of **1**–**8** in hand, it implied that each subtype *seco*-sativene sesquiterpenoids had a diagnostic daughter ion in the MS profile (subtype **A** → *m/z* 175; subtypes **B**/**D** → *m/z* 189; subtype **C** → *m/z* 203; subtype **E** → *m/z* 187). Though both subtypes **B** and **D** had the same diagnostic daughter ion *m/z* 189, the last cleavage in the sub-type **B** was the neutral loss of one molecule of CO (−28), whereas the neutral loss of one molecule of H_2O (−18) was the last cleavage in subtype **D**, which differentiated these two subtypes **B** and **D**. Thus, it could give the possible subtype of *seco*-sativene sesquiterpenoids based on the diagnostic daughter ion from the corresponding ESI-Q-TOF-MS/MS data.

Then, the crude extract of the ethyl acetate fraction of the plant pathogen *Bipolaris sorokiniana* was then analyzed by UPLC-Q-TOF-MS/MS (**Supplementary Figure 11**). There were some peaks (compound **8**: *m/z* 251.1664, t_R = 3.53 min, λ_{max} = 217 nm; compound **7**: *m/z* 225.1843, t_R = 3.56 min, λ_{max} = 206 nm; compound **2**: *m/z* 253.1797, t_R = 4.86 min, λ_{max} = 244 nm; compound **1**: *m/z* 249.1548, t_R = 4.93 min, λ_{max} = 248 nm; compound **3**: *m/z* 295.1900, t_R = 8.24 min, λ_{max} = 243 nm) in the TOF MS profiles possessing typical fragment ions including *m/z* 175, 187, 189, 203, 205, 207, 215, 217, 231, 233, and 235. However, there are other unidentified compounds (251.1639, t_R = 2.85 min; 353.0418, t_R = 5.78 min; 237.1855, t_R = 5.88 min; 293.1748, t_R = 7.03 min; 207.1744, t_R = 7.26 min; 235.1693, t_R = 7.86 min; 235.1693, t_R = 8.68 min; 235.1692, t_R = 8.85 min) that had similar cleavage fragments as compounds **1**–**8**, indicating that many known and undescribed analogues existed in the extract.

Compounds **1** (t_R = 4.93 min) and **2** (t_R = 4.86 min) as the main constituents were isolated from the plant pathogen *Bipolaris sorokiniana* crude extract.

Two ions (t_R = 7.23, 7.01 min) at *m/z* 267 $[M+1]^+$ (**9**) and *m/z* 293 $[M+1]^+$ (**10**) were detected in the crude extract, and their molecular weights were determined to be $C_{16}H_{26}O_3$ and $C_{17}H_{24}O_4$, respectively (**Supplementary Figures 9, 10**). The diagnostic ions of **9** and **10** were *m/z* 189/187 and λ_{max} = 234/215 nm, respectively, implying that structures of **9** and **10** possessed the same subtypes as **7** and **8**. The UPLC-Q-TOF-MS/MS fragmentation pathways of these two compounds were nearly the same as those of **7** and **8**, except for an additional acetyl group. To confirm this hypothesis, **9** and **10** were isolated from the extract and elucidated by IR, NMR, and HR-ESI-MS spectra. The IR absorption bands at 3,420 cm^{-1} showed the hydroxyl group in **9**, and 2,931 and 1,747 cm^{-1} revealed the presence of alkyl and ester moieties, respectively, which were also present in that of **10**. The ^{1}H-NMR spectrum revealed the similarity of **9**/**10** with **7**/**8**, except that the chemical shift values of $-CH_2$-12 of **9** and $-CH_2$-14 of **10** were down-fielded in **9**/**10** (Osterhage et al., 2002) and an additional methyl signal was observed in the ^{1}H-NMR spectrum of **9**/**10**. This implied that the additional acetyl group was connected at C-12 in **9**

TABLE 5 | Elemental constituents of major product ions from $[M+Na]^+$ for compound **7** (subtype D).

Fragment ion	Formula	Calculated	Observed	Error (PPM)
$[M+Na]^+$	$C_{14}H_{24}O_2Na$	247.1674	247.1668	−2.4
$[M+H]^+$	$C_{14}H_{25}O_2$	225.1855	225.1843	−5.3
$[M+H-H_2O]^+$	$C_{14}H_{23}O$	207.1749	207.1754	+2.4
$[M+H-2H_2O]^+$	$C_{14}H_{21}$	189.1643	189.1640	−1.6

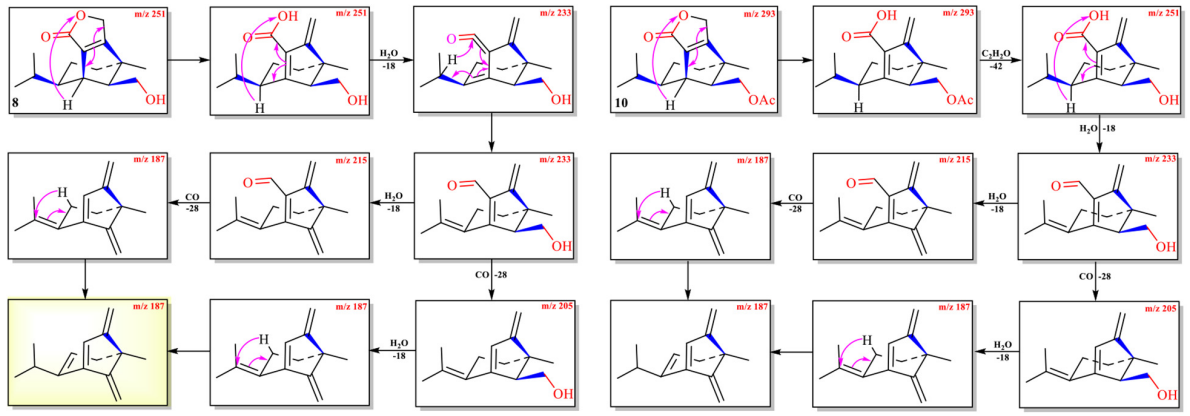

SCHEME 5 | Possible fragmentation pathways of **8** and **10**.

and C-14 in **10**. The key HMBC correlations from $-CH_2$-12/CH_2-14 and 1′-Me to C-2′ (δ_C 171.2 in **9**/**10**) supported the conclusion (**Figure 2** and **Supplementary Figures 12–29**). Thus, the structures of **9** and **10** were determined, and their ESI-Q-TOF-MS/MS fragmentation pathways were consistent with those of **7**/**8** (**Schemes 4**, **5** and **Supplementary Tables 4, 5**).

Antioxidant Activity

The antioxidant activities of compounds **1** and **2** were evaluated by the DPPH and $ABTS^+$ free radical scavenging test, and the results were presented as IC_{50} values. The results demonstrated that compound **1** displayed moderate antioxidant activities with IC_{50} of 0.90 and 1.97 mM for DPPH and $ABTS^+$ scavenging capacity, respectively. However, compound **2** did not show the obvious antioxidant activity. They were measured by comparing the scavenging ability of DPPH free radical and $ABTS^+$ free radical with V_C, a well-known potent antioxidant and free radical scavenger with IC_{50} of 0.14 and 0.42 mM for DPPH and $ABTS^+$ scavenging capacity, respectively (**Table 7**).

DISCUSSION

This report analyzed the fragmentation patterns of eight representative *seco*-sativene sesquiterpenoids (**1**–**8**) using UPLC-Q-TOF-MS/MS, and McLafferty rearrangement, 1,3-rearrangement, and neural loss (−18, −28) were the main fragmentation patterns. The results indicated that dehydration (−18) occurred easily in *seco*-sativenes with strong abundance of dehydration peak observed in **1**-**8**, and similar reports were found in other studies (McLafferty and Gohike, 1959; Alén, 1987; Nawamaki and Kuroyanagi, 1996; Sun et al., 2012; Giri et al., 2017; Qian et al., 2018). This may be due to an electron impact inducing fragmentations of alkene monocarboxylic acids to form an active OH ion, which combines an available methyl-hydrogen atom to one lost molecule of H_2O (−18) through the McLafferty rearrangement in a six-membered system (Baldas et al., 1969; Alexander et al., 1972). The molecular ion peak $[M+H]^+$ of **1**–**7** and **9** was not easily observed in the UPLC-Q-TOF-MS/MS profile, whereas $[M+Na]^+$ and $[M+H\text{-}H_2O]^+$ abundances of these compounds were relatively strong. As there was a characteristic 40 Da difference between $[M+Na]^+$ and $[M+H\text{-}H_2O]^+$, the molecular ion peak of **1**–**7** and **9** can be inferred. Compounds **8** and **10** possess a lactone ring at C-1 and C-2, which is different from **1**–**7** and **9**. The special group in **8** and **10** leads to their molecular ion peaks $[M+H]^+$ easily being observed in MS profiles. This might be a key signal for differentiating subtype E from other subtypes. Although the McLafferty rearrangement together with 1,3-rearrangement in alkene monocarboxylic molecules to produce a base peak of dehydration has been reported, this was the first report in *seco*-sativene sesquiterpenoids mass analysis, which provided a base for the *seco*-sativenes structural elucidation.

Diagnostic daughter ions of five subtypes of *seco*-sativene sesquiterpenoids were provided base on UPLC-Q-TOF-MS/MS analysis in this report. Subtypes A, B/D, and E possessed diagnostic daughter ions at *m*/*z* 175, 189, and 203, respectively, whereas subtype C showed a characteristic daughter ion at *m*/*z* 187 in the UPLC-Q-TOF-MS/MS profiles. The main difference between subtypes B and D was that the last cleavage was the neutral loss of one molecule of CO (−28) in subtype B, not the neutral loss of one molecule of H_2O (−18) in subtype D. Diagnostic ions provided signals for the different subtypes of *seco*-sativenes, and the rearrangement and neutral loss (H_2O, CO, and HOAc) in the fragmentation patterns provided the possible groups on the structures of *seco*-sativene sesquiterpenoids.

TABLE 6 | Elemental constituents of major product ions from $[M+Na]^+$ for compound **8** (subtype E).

Fragment ion	Formula	Calculated	Observed	Error (PPM)
$[M+Na]^+$	$C_{15}H_{22}O_3Na$	273.1467	273.1461	−2.2
$[M+H]^+$	$C_{15}H_{23}O_3$	251.1647	251.1664	+6.8
$[M+H\text{-}H_2O]^+$	$C_{15}H_{21}O_2$	233.1542	233.1536	−2.6
$[M+H\text{-}2H_2O]^+$	$C_{15}H_{19}O$	215.1436	215.1426	−4.6
$[M+H\text{-}H_2O\text{-}CO]^+$	$C_{14}H_{21}O$	205.1592	205.1585	−3.4
$[M+H\text{-}2H_2O\text{-}CO]^+$	$C_{14}H_{19}$	187.1487	187.1478	−4.8

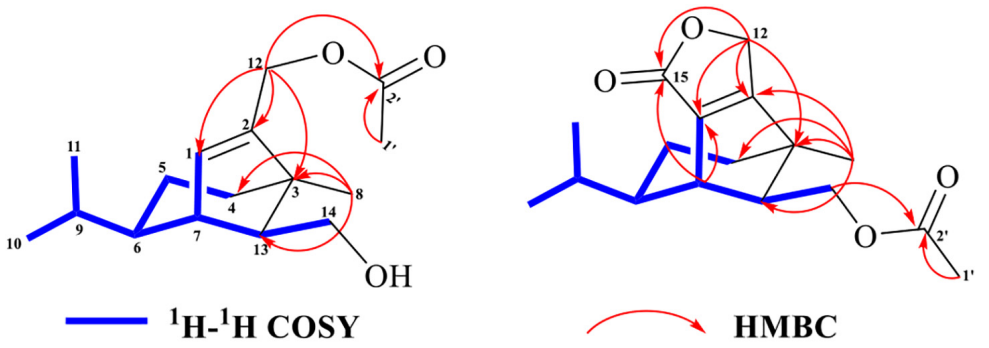

FIGURE 2 | Key 2D-NMR correlations of **9** and **10**.

Thus, the structures of the *seco*-sativenes could be inferred by fragmentation patterns combined with the diagnostic ions and molecular formula based on the UPLC-Q-TOF-MS/MS profile. This report provides a reliable method for the structural analysis of *seco*-sativene sesquiterpenoids.

Compounds **1**, **2**, **9**, and **10** and other *seco*-sativenes are a class of phytotoxins. Compound **1** was previously isolated from *C. sativus* (teleomorph: *B. sorokiniana*) without phytotoxicity on corn leaves, but helminthosporal acid with an aldehyde group at C-1 (a carboxyl group at C-1 in **1**) possessed strong phytotoxic activity (Li et al., 2020a). Therefore, the aldehyde group in helminthosporal acid might be a potential active group for phytotoxicity. Compound **2** exhibited bidirectional regulation activities. On the one hand, it was the gibberellin-like plant growth regulator, which could promote the growth of plant roots and leaves at low concentrations (Qader et al., 2017; Li et al., 2020a). On the other hand, it showed phytotoxicity on corn leaves (Li et al., 2020a). Compounds **9** and **10** did not show obvious antioxidant activity in this report, and no more activities of **9** and **10** were tested due to limited amounts. Compared with **7** and **8**, **9** and **10** possess an extra acetyl group at 12-OH and 5-OH, respectively. Osterhage et al. reported that **7** showed inhibitory activity against tyrosine kinase p56, *Microbotryum violaceum*, *Eurotium repens*, and *Escherichia coli* (Osterhage et al., 2002) and that **8** showed antifungal activity against *M. violaceum* (Osterhage et al., 2002) and phytotoxicity on corn leaves (Li et al., 2020a). Several reports suggested that 5-CH_2OH might be the potent active group of *seco*-sativenes sesquiterpenoids for their phytotoxicity (Nakajima et al., 1994; Li et al., 2020b). Therefore, **9** might possess phytotoxicity against barley seeds and corn leaves. But their structure–activity relationships (SARs) need to be further studied. At present, the reports on the activities of *seco*-sativene sesquiterpenoids mainly focused on phytotoxicity and growth-promoting effects with few reports about other activities (Li et al., 2020b). To further explore the medicinal value of *seco*-sativenes, the antioxidant activity of these compounds (**1**, **2**, **9**, and **10**) were studied in this report. Only then did compound **1** show moderate activity on DPPH scavenging capacity, which indicated that 13-COOH might be a possible active group, and further biological exploration should be needed in the future.

TABLE 7 | DPPH and $ABTS^+$ scavenging capacity of compounds **1**, **2**, **9**, and **10**.

Compound	DPPH (IC_{50})	$ABTS^+$ (IC_{50})
1	0.90 ± 0.17 mM	>1 mM
2	>1 mM	>1 mM
9	>1 mM	>1 mM
10	>1 mM	>1 mM
Vc	0.14 ± 0.05 mM	0.42 ± 0.30 mM

UPLC-Q-TOF-MS/MS spectrometry has evolved to be a mature and common technique, which is now widely used to analyze secondary metabolites from diverse biological resources. Most of researchers used this technology to identify (new/novel) metabolites or dereplicate in different crude extracts (Jin et al., 2018; Wang et al., 2020). Recently, a molecular networking technique based on (U)HPLC-MS/MS combined with different databases was used in the dereplication and targeting of new natural products from diverse biological resources (Watrous et al., 2012; Yang et al., 2013; Aksenov et al., 2017; Hou et al., 2019; Ramos et al., 2019; Rivera-Chaìvez et al., 2019; Shi et al., 2019; Wu et al., 2019; Chao et al., 2020; Zang et al., 2020; Lei et al., 2021; Lin et al., 2021). The molecular networking technique used the known or new compound as the "seed" to realize the visualization of analogues. In the network, MS data were collected from LC-MS and uploaded to the GNPS database for data processing to produce total molecular network profiles. Every node in the same network represented a compound possessing the same core skeleton. Known or new analogues can be quickly inferred according to molecular weight, molecular formula, and fragmentation patterns based on node analysis through searching different databases or house libraries. The targeted isolation of the seed analogues could be realized by searching the location of the "seed" (Klitgaard et al., 2015; Allard et al., 2016; Trautman and Crawford, 2016; Naman et al., 2017; Olivon et al., 2017a,b; Nothias et al., 2018). When a molecular network is combined with fragmentation patterns, the range of metabolites would be narrowed, and the precision of targeted-isolation-compounds would be improved (He et al., 2021). Thus, molecular networking based on the (U)HPLC-MS/MS technique would provide a more convenient approach for dereplication and targeting-isolation of new *seco*-sativene sesquiterpenoids in the future.

CONCLUSION

Eight *seco*-sativene sesquiterpenoids (**1**–**8**) were analyzed using the UPLC-Q-TOF-MS/MS technique in positive mode, from which their possible mass fragmentation patterns were suggested, and neural loss, McLafferty rearrangement, and 1,3-rearrangement were the main clearage patterns. These eight *seco*-sativene sesquiterpenoids (**1**–**8**) were summarized to be five subtypes according to their structural features. Each subtype possessed a diagnostic daughter ion, which, in return, could contribute to the elucidation of *seco*-sativene sesquiterpenoids. Based on the fragmentation mechanism mentioned above, some analogues including two potentially new ones were detected. Two known (**1** and **2**) and two new analogues (**9** and **10**) were then isolated from the extract of the plant pathogen *Bipolaris sorokiniana*. Their structures were elucidated mainly by NMR spectra and supported based on their UPLC-Q-TOF-MS/MS analysis. The results demonstrated that diagnostic mass ions of *seco*-sativene sesquiterpenoids in the UPLC-Q-TOF-MS/MS profiles provided a convenient and high-performance approach for structural characterization and also support that UPLC-Q-TOF-MS/MS is a powerful and sensitive tool for dereplication and detection of new analogues in crude extracts. This study will pave the way for the structural analysis and targeting isolation of *seco*-sativene sesquiterpenoids in different fungal crude extracts.

DATA AVAILABILITY STATEMENT

The original contributions presented in the study are included in the article/**Supplementary Material**, further inquiries can be directed to the corresponding author/s.

AUTHOR CONTRIBUTIONS

Y-DW, JY, and GD: experiment and writing – review and editing. Y-DW, JY, Y-YL, X-MT, and QL: data collection. S-YY and S-BN: activity experiment. HD: resources. JY, GD, and L-PG: funding acquisition. GD and Y-DW: writing – original draft preparation. All authors have read and agreed to the published version of the manuscript.

FUNDING

We gratefully acknowledge financial support from the National Natural Science Foundation of China (81891014), the National Key R&D Programme of China (2017YFC1700701), the Key Project at Central Government Level: Establishment of the sustainable use for valuable Chinese Medicine Resources (2060302), and the Fundamental Research Funds for the Central public welfare research institutes (ZZXT201906).

ACKNOWLEDGMENTS

We gratefully acknowledge Jin-wei Ren for kindly helping to measure the NMR spectra.

SUPPLEMENTARY MATERIAL

The Supplementary Material for this article can be found online at: https://www.frontiersin.org/articles/10.3389/fmicb.2022.807014/full#supplementary-material

REFERENCES

Ahad, H., Jin, H., and Liu, Y. (2020). Chemical profiling of spermidines in goji berry by strong cation exchange solid-phase extraction (SCX-SPE) combined with ultrahigh-performance liquid chromatography-quadrupole time-of-flight mass spectrometry (UPLC-Q-TOF/MS/MS). *J. Chromatogr. B.* 1137, 121923. doi: 10.1016/j.jchromb.2019.121923

Aksenov, A. A., da Silva, R., and Knight, R. (2017). Global chemical analysis of biology by mass spectrometry. *Nat. Rev. Chem.* 1, 1–20.

Alén, R. (1987). Formation of acid-catalysed dehydration products from xyloisosaccharinic acid. *Acta chem. Scand. Ser. B. Org. Chem. Biochem.* 41, 76–78.

Alexander, R. G., Bigley, D. B., and Todd, J. F. J. (1972). Mass spectral studies of unsaturated carboxylic acids-I: some cyclic and acyclic βγ−unsaturated acids. *Org. Mass Spectrom.* 6, 1153–1160.

Ali, L., Khan, A. L., Hussain, J., Al-Harrasi, A., Waqas, M., Kang, S. M., et al. (2016). Sorokiniol: a new enzymes inhibitory metabolite from fungal endophyte *Bipolaris sorokiniana* LK12. *BMC Microbiol.* 16:103. doi: 10.1186/s12866-016-0722-7

Allard, P. M., Peìresse, T., Bisson, J., Gindro, K., Marcourt, L., Pham, V. C., et al. (2016). Integration of molecular networking and in-silico MS/MS fragmentation for natural products dereplication. *Anal. Chem.* 88, 3317–3323. doi: 10.1021/acs.analchem.5b04804

Baldas, J., Porter, Q. N., and Ramsay, C. C. R. (1969). Mass spectrometric studies. V. Benzylidenemalonic acid and related compounds. *Aust. J. Chem.* 22, 405–422.

Briggs, D. E. (1966). Gibberellin-like activity of helminthosporol and helminthosporic acid. *Nature.* 210, 418–419.

Chao, R., Hou, X. M., Xu, W. F., Hai, Y., Wei, M. Y., Wang, C. Y., et al. (2020). Targeted Isolation of Asperheptatides from a coral-derived fngus using LC-MS/MS-based molecular networking and antitubercular activities of modified cnnamate derivatives. *J. Nat. Prod.* 84, 11–19. doi: 10.1021/acs.jnatprod.0c00804

Chen, C., Xue, Y., and Li, Q. M. (2018). Neutral loss scan-based strategy for integrated identification of amorfrutin derivatives, new peroxisome proliferator-activated receptor gamma agonists, from *Amorpha Fruticosa* by UPLC-QqQ-MS/MS and UPLC-Q-TOF-MS. *J. Am. Soc. Mass Spectrom.* 29, 685–693. doi: 10.1007/s13361-018-1891-4

Conceição, R. S., Reis, I. M. A., Cerqueira, A. P. M., Perez, C. J., Junior, M. C. D. S., Branco, A., et al. (2020). Rapid structural characterisation of benzylisoquinoline and aporphine alkaloids from *Ocotea spixiana* acaricide extract by HPTLC-DESI-MS^n. *Phytochem. Analysis.* 31, 711–721. doi: 10.1002/pca.2935

Giri, A., Coutriade, M., and Racaud, A. (2017). Molecular characterization of volatiles and petrochemical base oils by photo-ionization GC× GC-TOF-MS. *Anal. Chem.* 89, 5395–5403. doi: 10.1021/acs.analchem.7b00124

Hashimoto, T., Sakurai, A., and Tamura, S. (1967). Physiological activities of helminthosporol and helminthosporic acid: I. Effects on growth of intact plants. *Plant Cell Physiol.* 8, 23–34.

He, Q. F., Wu, Z. L., Li, L., Sun, W. Y., Wang, G. Y., Jiang, R. W., et al. (2021). Discovery of neuritogenic securinega alkaloids from *Flueggea suffruticosa* by a

building blocks-based molecular network strategy. *Angew. Chem. Int. Ed.* 60, 19609–19613. doi: 10.1002/anie.202103878

Hou, X. M., Li, Y. Y., Shi, Y. W., Fang, Y. W., Chao, R., Gu, Y. C., et al. (2019). Integrating molecular networking and 1H NMR to target the isolation of chrysogeamides from a library of marine-derived Penicillium fungi. *J. Org. Chem.* 84, 1228–1237. doi: 10.1021/acs.joc.8b02614

Jin, M., Zhang, W., Jiang, H., Du, Y. F., Guo, W., Cao, L., et al. (2018). UPLC-Q-TOF-MS/MS-guided dereplication of *Pulsatilla chinensis* to identify triterpenoid saponins. *Phytochem. Analysis.* 29, 516–527. doi: 10.1002/pca.2762

Katsumi, M., Tamura, S., and Sakurai, A. (1967). Gibberellin-like activity of helminthosporol, helminthosporic acid and dihydrohelminthosporic acid in leaf sheath elongation of dwarf 5 mutants of Zea mays. *Naturwissenschaften.* 54, 96–97.

Klitgaard, A., Nielsen, J. B., and Frandsen, R. J. (2015). Combining stable isotope labeling and molecular networking for biosynthetic pathway characterization. *Anal. Chem.* 87, 6520–6526. doi: 10.1021/acs.analchem.5b01934

Lei, H., Zhang, Y., Zu, X., Ye, J., Liang, Y., Cheng, T., et al. (2021). Comprehensive profiling of the chemical components and potential markers in raw and processed *Cistanche tubulosa* by combining ultra-high-performance liquid chromatography coupled with tandem mass spectrometry and MS/MS-based molecular networking. *Anal. Bioanal. Chem.* 413, 129–139. doi: 10.1007/s00216-020-02983-0

Li, Y. Y., Tan, X. M., Wang, Y. D., Yang, J., Zhang, Y. G., Sun, B. D., et al. (2020a). Bioactive seco-sativene sesquiterpenoids from an *Artemisia desertorum* endophytic fungus, *Cochliobolus sativus*. *J. Nat. Prod.* 85, 1488–1494. doi: 10.1021/acs.jnatprod.9b01148

Li, Y. Y., Tan, X. M., Yang, J., Guo, L. P., and Ding, G. (2020b). Naturally Occurring *seco*-sativene sesquiterpenoid: chemistry and biology. *J. Agric. Food Chem.* 68, 9827–9838. doi: 10.1021/acs.jafc.0c04560

Liang, Y., Yan, G. Y., Wu, J. L., Zong, X., Liu, Z., Zhou, H., et al. (2018). Qualitative and quantitative analysis of lipo-alkaloids and fatty acids in *Aconitum carmichaelii* using LC-MS and GC-MS. *Phytochem. Analysis.* 29, 398–405. doi: 10.1002/pca.2760

Lin, X., Chai, L., Zhu, H. R., Zhou, Y., Shen, Y., Chen, K. H., et al. (2021). Applying molecular networking for targeted isolation of depsipeptides. *RSC Advances* 11, 2774–2782. doi: 10.1039/d0ra09388b

Ludwig, R. A. (1957). Toxin production by *Helminthosporium sativum* and its significance in disease development. *Can. J. Bot.* 35, 291–303. doi: 10.1139/b57-026

Ludwig, R. A., Clark, R. V., and Julien, J. B. (1956). Studies on the seedling disease of barley caused by *Helminthosporium sativum*. *Can. J. Bot.* 34, 653–673. doi: 10.1139/b56-048

Mayo, P. D., and Williams, R. E. (1965). Sativene, parent of the toxin from *Helminthosporium sativum*. *J. Am. Chem. Soc.* 87, 3275. doi: 10.1021/ja01092a066

Mayo, P. D., Robinson, J. R., and Spencer, E. Y. (1962a). The biogenesis of helminthosporal. *Experientia.* 18, 359–360. doi: 10.1007/bf02172248

Mayo, P. D., Spencer, E. Y., and White, R. W. (1961). Helminthosporal, the toxin from *Helminthosporium sativum*: I. Isolation and characterization. *Can. J. Chem.* 39, 1608–1612. doi: 10.1139/v61-205

Mayo, P. D., Spencer, E. Y., and White, R. W. (1962b). The constitution of helminthosporal. *J. Am. Chem. Soc.* 84, 494–495. doi: 10.1021/ja00862a037

Mayo, P. D., Spencer, E. Y., and White, R. W. (1963). Terpenoids: IV. The structure and stereochemistry of helminthosporal. *Can. J. Chem.* 41, 2996–3004. doi: 10.1139/v63-440

Mayo, P. D., Williams, R. E., and Spencer, E. Y. (1965). Terpenoids: VIII. The immediate precursors of helminthosporal and helminthosporol. *Can. J. Chem.* 43, 1357–1365. doi: 10.1139/v65-184

McLafferty, F. W., and Gohike, R. S. (1959). Mass spectrometric analysis. Aromatic acids and esters. *Anal. Chem.* 31, 2076–2082. doi: 10.1021/ac60156a062

Miyazaki, S., Jiang, K., Kobayashi, M., Asami, T., and Nakajima, M. (2017). Helminthosporic acid functions as an agonist for gibberellin receptor. *Biosci. Biotechnol. Biochem.* 81, 2152–2159. doi: 10.1080/09168451.2017.1381018

Miyazaki, S., Tomita, K., Yamane, H., Kobayashi, M., Asami, T., and Nakajima, M. (2018). Characterization of a helminthosporic acid analog that is a selective agonist of gibberellin receptor. *Bioorg. Med. Chem. Lett.* 28, 2465–2470. doi: 10.1016/j.bmcl.2018.06.005

Nakajima, H., Isomi, K., and Hamasaki, T. (1994). Sorokinianin: a novel phytotoxin produced by the phytopathogenic fungus *Bipolaris sorokiniana*. *Tetrahedron Lett.* 35, 9597–9600. doi: 10.1016/0040-4039(94)88520-6

Naman, C. B., Rattan, R., and Nikoulina, S. E. (2017). Integrating molecular networking and biological assays to target the isolation of a cytotoxic cyclic octapeptide, samoamide A, from an American Samoan marine cyanobacterium. *J. Nat. Prod.* 80, 625–633. doi: 10.1021/acs.jnatprod.6b00907

Nawamaki, K., and Kuroyanagi, M. (1996). Sesquiterpenoids from *Acorus calamus* as germination inhibitors. *Phytochem.* 43, 1175–1182. doi: 10.1016/s0031-9422(96)00401-3

Nihashi, Y., Lim, C. H., Tanaka, C., Miyagawa, H., and Ueno, T. (2002). Phytotoxic sesterterpene, 11-epiterpestacin, from *Bipolaris sorokiniana* NSDR-011. *Biosci. Biotechnol. Biochem.* 66, 685–688. doi: 10.1271/bbb.66.685

Nothias, L. F., Nothias-Esposito, M., and da Silva, R. (2018). Bioactivity-based molecular networking for the discovery of drug leads in natural product bioassay-guided fractionation. *J. Nat. Prod.* 81, 758–767. doi: 10.1021/acs.jnatprod.7b00737

Nukina, M., Hattori, H., and Marumo, S. (1975). Cis-Sativenediol, a plant growth promotor, produced by fungi. *J. Am. Chem. Soc.* 97, 2542–2543.

Olivon, F., Allard, P. M., Koval, A., Righi, D., Genta-Jouve, G., Neyts, J., et al. (2017a). Bioactive natural products prioritization using massive multi-informational molecular networks. *ACS Chem. Biol.* 12, 2644–2651. doi: 10.1021/acschembio.7b00413

Olivon, F., Grelier, G., Roussi, F., Litaudon, M., and Touboul, D. (2017b). MZmine 2 data-preprocessing to enhance molecular networking reliability. *Anal. Chem.* 89, 7836–7840. doi: 10.1021/acs.analchem.7b01563

Osterhage, C., König, G. M., and Höller, U. (2002). Rare sesquiterpenes from the algicolous fungus *Drechslera dematioidea*. *J. Nat. Prod.* 65, 306–313. doi: 10.1021/np010092l

Pena-Rodriguez, L. M., and Chilton, W. S. (1989). Victoxinine and prehelminthosporolactone, two minor phytotoxic metabolites produced by *Bipolaris* sp., a pathogen of Johnson grass. *J. Nat. Prod.* 52, 899–901. doi: 10.1021/np50064a046

Pena-Rodriguez, L. M., Armingeon, N. A., and Chilton, W. S. (1988). Toxins from weed pathogens, I. Phytotoxins from a bipolaris pathogen of johnson grass. *J. Nat. Prod.* 51, 821–828. doi: 10.1021/np50059a001

Phan, C. S., Li, H., Kessler, S., Solomon, P. S., Piggott, A. M., and Chooi, Y. H. (2019). Bipolenins K–N: New sesquiterpenoids from the fungal plant pathogen *Bipolaris sorokiniana*. *Beilstein. J. Org. Chem.* 15, 2020–2028. doi: 10.3762/bjoc.15.198

Qader, M. M., Kumar, N. S., Jayasinghe, L., Araya, H., and Fujimoto, Y. (2017). Bioactive sesquiterpenes from an endophytic fungus *Bipolaris sorokiniana* isolated from a popular medicinal plant Costus speciosus. *Mycology* 8, 17–20.

Qian,H., Yu, F. J., and Lu, D. Y. (2018). Identification of poliumoside metabolites in rat plasma, urine, bile, and intestinal bacteria with UPLC/Q-TOF-MS. *Chin. J. Nat. Med.* 16, 871–880. doi: 10.1016/S1875-5364(18)30129-8

Ramos, A. E. F., Evanno, L., Poupon, E., Champy, P., and Beniddir, M. A. (2019). Natural products targeting strategies involving molecular networking: different manners, one goal. *Nat. Prod. Rep.* 36, 960–980. doi: 10.1039/c9np00006b

Rivera-Chaìvez, J., Zacatenco-Abarca, J., and Morales-Jimeìnez, J. (2019). Cuautepestalorin, a 7, 8-dihydrochromene–oxoisochromane adduct bearing a hexacyclic scaffold from *Pestalotiopsis* sp. IQ-011. *Org. lett.* 21, 3558–3562. doi: 10.1021/acs.orglett.9b00962

Scupinari, T., Mannochio Russo, H., and Sabino Ferrari, A. B. (2020). Crotalaria spectabilis as a source of pyrrolizidine alkaloids and phenolic compounds: HPLC-MS/MS dereplication and monocrotaline quantification of seed and leaf extracts. *Phytochem. Analysis.* 31, 747–755. doi: 10.1002/pca.2938

Shi, Y., Gu, R., Li, Y., Wang, X., Ren, W., and Li, X. (2019). Exploring novel herbicidin analogues by transcriptional regulator overexpression and MS/MS molecular networking. *Microb. Cell Factories* 18, 1–17. doi: 10.1186/s12934-019-1225-7

Spencer, E. J. (1965). World review of pest control. *Bulletin of the Entomological Society of America* 4, 75.

Sun, B. S., Xu, M. Y., and Li, Z. (2012). UPLC-Q-TOF-MS/MS analysis for steaming times-dependent profiling of steamed Panax quinquefolius and its ginsenosides transformations induced by repetitious steaming. *J. Ginseng. Res.* 36, 277. doi: 10.5142/jgr.2012.36.3.277

Taniguchi, E., and White, G. A. (1967). Site of action of the phytotoxin, helminthosporal. *Biochem. Biophys. Res. Commun.* 28, 879–885. doi: 10.1016/0006-291x(67)90060-5

Trautman, E., and Crawford, M. (2016). Linking biosynthetic gene clusters to their metabolites via pathway-targeted molecular networking. *Curr. Top. Med. Chem.* 16, 1705–1716. doi: 10.2174/1568026616666151012111046

Wang, F., Huang, S., Chen, Q., Hu, Z., Li, Z., Zheng, P., et al. (2020). Chemical characterisation and quantification of the major constituents in the Chinese herbal formula Jian-Pi-Yi-Shen pill by UPLC-Q-TOF-MS/MS and HPLC-QQQ-MS/MS. *Phytochem. Anal.* 31, 915–929. doi: 10.1002/pca.2963

Watrous, J., Roach, P., and Alexandrov, T. (2012). Mass spectral molecular networking of living microbial colonies. *Proc. Natl. Acad. Sci. USA.* 109, E1743–E1752. doi: 10.1073/pnas.1203689109

White, G., and Taniguchi, E. (1972). The mode of action of helminthosporal. II. Effect on the permeability of plant cell membranes. *Can. J. Bot.* 50, 1415–1420.

Wu, C., van der Heul, H. U., and Melnik, A. V. (2019). Lugdunomycin, an Angucyline-drived molecule with unprecedented chemistry architecture. *Angew. Chem. Int. Ed.* 131, 2835–2840. doi: 10.1002/anie.201814581

Yang, J. Y., Sanchez, L. M., and Rath, C. M. (2013). Molecular networking as a dereplication strategy. *J. Nat. Prod.* 76, 1686–1699.

Yang, S., Shan, L., Luo, H., Sheng, X., Du, J., and Li, Y. (2017). Rapid classification and identification of chemical components of schisandra chinensis by uplc-q-tof/ms combined with data post-processing. *Molecules.* 22, 1778. doi: 10.3390/molecules22101778

Zang, Y., Gong, Y., and Gong, J. (2020). Fungal polyketides with three distinctive ring skeletons from the fungus *Penicillium canescens* uncovered by OSMAC and molecular networking strategies. *J. Org. Chem.* 85, 4973–4980. doi: 10.1021/acs.joc.0c00147

Conflict of Interest: The authors declare that the research was conducted in the absence of any commercial or financial relationships that could be construed as a potential conflict of interest.

Publisher's Note: All claims expressed in this article are solely those of the authors and do not necessarily represent those of their affiliated organizations, or those of the publisher, the editors and the reviewers. Any product that may be evaluated in this article, or claim that may be made by its manufacturer, is not guaranteed or endorsed by the publisher.